

EHT tests of the strong-field regime of General Relativity

Sebastian H. Völkel^{1,2,*}, Enrico Barausse^{1,2,†}, Nicola Franchini^{1,2,‡}, and Avery E. Broderick^{3,4,5§}

¹SISSA, Via Bonomea 265, 34136 Trieste, Italy and INFN Sezione di Trieste

²IFPU - Institute for Fundamental Physics of the Universe, Via Beirut 2, 34014 Trieste, Italy

³Department of Physics and Astronomy, University of Waterloo,
200 University Avenue West, Waterloo, ON N2L 3G1, Canada

⁴Perimeter Institute for Theoretical Physics, 31 Caroline Street North, Waterloo, ON N2L 2Y5, Canada

⁵Waterloo Centre for Astrophysics, University of Waterloo, Waterloo, ON N2L 3G1, Canada

(Dated: October 13, 2021)

Following up on a recent analysis by Psaltis *et al.* [Phys. Rev. Lett. 125, 141104 (2020)], we show that the observed shadow size of M87* can be used to unambiguously and robustly constrain the black hole geometry in the vicinity of the circular photon orbit. Constraints on the post-Newtonian weak-field expansion of the black hole's metric are instead more subtle to obtain and interpret, as they rely on combining the shadow-size measurement with suitable theoretical priors. We provide examples showing that post-Newtonian constraints resulting from shadow-size measurements should be handled with extreme care. We also discuss the similarities and complementarity between the EHT shadow measurements and black-hole gravitational quasi-normal modes.

Until the LIGO/Virgo detection of gravitational waves (GWs) [1–9], General Relativity (GR) had only been tested in the solar system (characterized by weak gravitational fields and mildly relativistic velocities v) [10] and in binary pulsars (which have strong gravitational fields inside/near the two stars, but again mildly relativistic orbital velocities v) [11]. Since in both cases $v \ll c$, these tests are normally performed within the post-Newtonian formalism (i.e. an expansion in powers of v/c) [12]. The advent of GW astronomy has pushed these tests to the strong-field *and* highly relativistic regime that characterizes merging BH binaries [13–15], where the PN formalism breaks down (except in the early-inspiral phase).

After coalescence, the BH merger remnant is expected to “ring down” by emitting quasi-normal modes (QNMs) [16–18], i.e. damped oscillations with discrete frequencies and damping times, functions of the BH mass and spin only (because of the no-hair theorem [19–22]). Therefore, by measuring two QNMs, one can in principle test the no-hair theorem and thus GR [18, 23]. These tests are not yet possible with current detectors [24] (even though there are clues of a second mode – and namely the first overtone of the dominant mode – besides the dominant QNM [25]). However, comparatively weaker inspiral-ringdown self-consistency tests, which compare the post-merger data to the signal predicted by GR by extrapolating the inspiral, show currently no hints of deviations from binary BHs in GR [13–15].

On larger scales, Psaltis *et al.* [26] proposed using the shadow size of M87* to constrain deviations of the BH geometry from GR (i.e. to test the no-hair theorem). The EHT shadow-size measurement is consistent (to within 17% at 68-percentile confidence level) with the GR prediction¹ based on the object's mass-to-distance ratio de-

rived from stellar dynamics [26, 30, 31]. Therefore, [26] concludes that theories extending/modifying GR cannot yield shadow sizes differing by more than 17% (at 68% confidence) from the GR (i.e. Schwarzschild/Kerr) prediction [26].²

While this idea is not new [33–45], Psaltis *et al.* [26] used it to constrain the BH geometry at 2PN order and beyond. To allow for deviations of the BH geometry from the Schwarzschild/Kerr solutions of GR, [26] utilizes parametrized metrics [46–50] that yield the usual PN expansion far from the BH, but which might be valid also in the strong-field region, where the PN expansion fails. [26] also assumes that *only one* of the parameters that regulate deviations from GR in these metrics is non-zero and allowed to vary.

We will show that bounds on PN coefficients such as those obtained by [26] depend sensitively on the assumed form of the parametrized BH metric. This is not surprising, as the results of [26] rely on a single measurement (the shadow's size). We will show instead that EHT shadow-size measurements can robustly constrain the BH geometry in the strong-field regime (near the circular photon orbit) and that these constraints are complementary to those from GW observations of QNMs.

Throughout this paper, we use units $G = c = 1$ and metric signature $-+++$.

EHT constraints on the PN expansion of BH geometry

photon sphere (i.e., for Schwarzschild BHs, the circular photon orbit). This is supported by simulations of the accretion flow onto M87* [27]. If this identification is not exact (see §5.3, 7.3, and Appendix D of [27], cf. [28, 29]), it will lead to larger errors in our analysis and in that of [26].

²This optimistically neglects possible correlations of the parameters regulating deviations from GR with those of the BH (mass and spin) and accretion flow, which are fixed in [26]. These correlations may be important, as shown e.g. in [32] for tests of GR with X-ray observations.

¹ Like [26], we assume that the shadow rim is associated with the

tries: As an example, we focus on the non-spinning parametrized geometry of Rezzolla and Zhidenko (RZ) [50] (see [51, 52] for the axisymmetric generalization).³ The g_{tt} component is

$$-g_{tt} = x \left(1 - \varepsilon(1-x) + (a_0 - \varepsilon)(1-x)^2 + \tilde{A}(x)(1-x)^3 \right), \quad (1)$$

with $x \equiv 1 - r_0/r$ (r_0 being the horizon's radius), and

$$\varepsilon = -\left(1 - \frac{2M}{r_0}\right), \quad \tilde{A}(x) = \frac{a_1}{1 + \frac{a_2 x}{1 + \frac{a_3 x}{1 + \dots}}}, \quad (2)$$

where M is the mass and the dots represent a continued fraction structure. The Schwarzschild limit is recovered when $\varepsilon, a_i \rightarrow 0$ (with $i = 0, 1, 2, 3, \dots$). When expanded in orders of $1/r$, one recovers the usual PN structure

$$-g_{tt} = 1 - \frac{2M}{r} + \sum_{i=1}^{\infty} P_i \left(\frac{M}{r} \right)^{i+1}, \quad (3)$$

where the parameters P_i depend on ε, a_i and vanish in the Schwarzschild limit. However, the continued-fraction structure of Eq. (2) is introduced to accelerate the convergence of the PN expansion (i.e. to “resum” it), so that the RZ metric aims to provide an accurate description even in the strong-field regime.

Null geodesics in a static, spherically symmetric geometry satisfy [53]

$$\frac{(g_{tt})^2}{E^2} \left(\frac{dr_*}{d\sigma} \right)^2 + V = 0, \quad (4)$$

$$V = -1 - \frac{b^2 g_{tt}}{r^2}, \quad (5)$$

where $dr_*/d\sigma$ is the derivative (with respect to an affine parameter σ) of the tortoise coordinate r_* (defined by $dr_*/dr = \sqrt{-g_{rr}/g_{tt}}$, with r the areal radius), and $b = L/E$ (with E and L the photon's conserved energy and angular momentum) is the impact parameter. The circular photon orbit's radius, r_{ph} , and its impact parameter, b_{ph} , correspond to a minimum of the effective potential, i.e. they solve $V = dV/dr = 0$. These conditions can be reduced to [26]

$$r_{\text{ph}} = \left(\frac{d}{dr} \ln \sqrt{-g_{tt}} \right)^{-1} \Big|_{r_{\text{ph}}}, \quad (6)$$

$$b_{\text{ph}} = \frac{r_{\text{ph}}}{\sqrt{-g_{tt}(r_{\text{ph}})}}, \quad (7)$$

which can be solved numerically for generic metrics; the Schwarzschild metric gives $r_{\text{ph}} = 3M$ and $b_{\text{ph}} = 3\sqrt{3}M$. If b_{ph} is interpreted as the measured shadow size (like in [26]), the EHT shadow-size measurement bounds $|b_{\text{ph}}/M - 3\sqrt{3}|/(3\sqrt{3}) \lesssim 0.17$ at 68% confidence [26].

The implications of this bound for the BH geometry depend on our prior knowledge of its functional form. For instance, if we assume Eq. (3) with all PN coefficients set to zero except for the 2PN term, i.e. $P_i = 0$ for $i \neq 2$ and flat priors for P_2 , one obtains the posterior distribution for P_2 shown in the first panel (left half) of Fig. 1. However, consider the RZ metric, imposing agreement with GR at 1PN order ($a_0 = 0$; we will comment on this assumption below) and setting $a_i = 0$ for $i \geq 4$ for simplicity. With the four non-zero parameters ε, a_1, a_2 and a_3 (for which we assume large flat priors of ± 30), the posterior distribution for

$$P_2 = -\frac{r_0^2}{M^2} \left[\left(-\frac{a_1(a_3+1)}{a_2+a_3+1} + 1 \right) \frac{r_0}{M} - 2 \right] \quad (8)$$

is extremely broad (first panel of Fig. 1, right half). Similar conclusions hold for the higher PN terms whose expressions we do not show as lengthy and uninformative. In the second and third panels of Fig. 1, we show similar bounds for the 3PN and 4PN coefficients P_3 and P_4 , both when they are considered optimistically as the only free parameters [one at a time, via the metric (3)], and when their posteriors are instead obtained from those of the parameters ε, a_1, a_2 and a_3 . All results of Fig. 1 were produced with the Metropolis-Hastings sampler of PyMC3 [54], assuming Gaussian errors on the EHT shadow-size measurement. The bounds of Fig. 1 are reminiscent of those presented in Fig. 7 of [13] by the LIGO/Virgo collaboration for the PN coefficients of the BH-binary inspiral GW signal.⁴ Indeed, our approach resembles closely that of [13], i.e. “optimistic” bounds are obtained by letting those PN coefficients free one by one, while “pessimistic” bounds assume that they are all allowed to vary simultaneously. We stress that correlations between the PN coefficients, when several of them are allowed to vary simultaneously, also appear in the case of GW measurements. However, unlike our case, the LIGO/Virgo “pessimistic” posteriors are smaller than the priors, at least for the leading-order (0PN) term in the GW phase, cf. Table I of [13] (see also [56–58]). This will be even more true for the -1PN term [14, 59]. Note also that the conclusions of our Fig. 1 (and namely that the “pessimistic” bounds on the single PN parameters—while marginalizing on all others—coincide with the pri-

³ We neglect the spin as our goal is to discuss the robustness of the M87* shadow-size constraints with respect to the parametrization of the non-GR effects.

⁴ See also [55] for GW bounds on the PN coefficients of the conservative dynamics, which are stronger than those claimed by [26] although comparable directly to them (because like [26], [55] assumes only one free non-GR parameter).

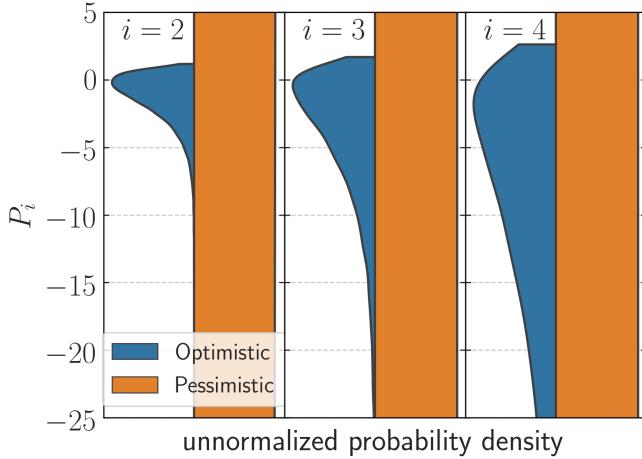


FIG. 1. Posteriors of the 2PN (left violin plot), 3PN (middle) and 4PN coefficients of the BH metric. The left half of each plot shows the “optimistic” bound obtained when only the term under consideration is allowed to deviate from GR, while the right half shows the posterior distribution for the same quantity, but in a parametrized metric with four parameters ϵ , a_1 , a_2 and a_3 . The sharp cutoff of the “optimistic” posteriors is *not* an artifact, and roughly corresponds to the metric ceasing to possess an event horizon. The “pessimistic” posteriors coincide with the priors.

ors) are robust against inclusion of lower-PN orders (e.g. P_1).

Fig. 1 shows that the bounds of [26] are not robust, but depend on the form of the parametrized metric and on the priors on its parameters. To illustrate how subtle it is to put priors on the shape and PN coefficients of parametrized metrics, let us stress that even though we have followed above [26] and required g_{tt} to match the Schwarzschild solution at 1PN order (i.e. $a_0 = P_1 = 0$), there is in principle no reason to do so. While [26] sets 1PN deviations from GR to zero, theories different from GR do not necessarily satisfy Birkhoff’s theorem [60] and may not obey the strong-equivalence principle [59]. Therefore, the metric around BHs need not be the same as around a star, and one cannot invoke solar-system tests to set the 1PN deviations from GR to zero. While this was mentioned in [26], the implications of the assumption of vanishing 1PN deviations from GR was not explored ([26] simply mentions that as a “very conservative” assumption). We will now explore cases where that assumption is not verified and affects the bounds that one obtains.

An example is given by a theory with a “dark photon” [i.e. a U(1) gauge field], possibly coupled with a scalar [61, 62]:

$$S = \int \frac{d^4x \sqrt{-g}}{16\pi} \left[R - \frac{1}{2} \nabla_a \phi \nabla^a \phi + e^{-\alpha_0 \phi} F_{ab} F^{ab} \right] \quad (9)$$

This is known as Einstein-Maxwell-dilaton theory [if the

U(1) symmetry is broken, e.g. by a light mass, the dark photon may even be the dark matter; cf. [63] and references therein]. Spherical BHs in this theory are described by a generalized Reissner-Nordström metric. The tt component reads [61, 64]

$$-g_{tt} = \left(1 - \frac{r_+}{\bar{r}}\right) \left(1 - \frac{r_-}{\bar{r}}\right)^{1-\alpha_1}, \quad (10)$$

where the areal radius is $r = \bar{r}(1 - r_-/\bar{r})^{\alpha_1/2}$, $\alpha_1 = 2\alpha_0^2/(1 + \alpha_0^2)$ and the constants r_\pm are related to the mass M and the dark charge Q of the BH through $2M = r_+ + (1 - \alpha_1)r_-$ and $2Q^2 = r_+r_-(2 - \alpha_1)$. Unlike an electric charge, which is neutralized by the plasma near the horizon [65], Q may be non-zero and different for a BH (where it is a free parameter) and a star (where it vanishes unless the dark photon and/or the scalar are coupled to the Standard Model). Obviously, for $Q \neq 0$ and $\alpha_1 \neq 1$ the metric (10) deviates from Schwarzschild at 1PN order.

EHT strong-field tests of gravity: We stress that the behavior of Fig. 1 – and namely the fact that the (marginalized) pessimistic bounds on the PN coefficients coincide with the priors – is not only due to the larger number of parameters being varied. In fact, irrespective of how many parameters the model (i.e. the parametrized metric) has, the shadow size does constrain a particular combination of the parameters. We show this explicitly in Fig. 2, where we plot the posteriors for g_{tt} and dg_{tt}/dr (evaluated at r_{ph}) in the “pessimistic” scenario of Fig. 1.⁵ This shows that the data *is* informative and that the inference can be robust against the number of parameters involved, as long as one asks the right question (i.e. as long as one does not attempt to estimate the PN coefficients, but focuses instead on the geometry near the circular photon orbit). Conversely, the geometry away from the circular photon orbit (even in its immediate vicinity) is less constrained, as shown by the posteriors at $r = 0.85r_{ph}$ and $r = 1.15r_{ph}$ plotted in Fig. 2. This plot therefore highlights that the behavior of the PN constraints of Fig. 1 is due to the slow convergence (if any) of PN expansion near the circular photon orbit.

As correctly stated in [26], “if more than one PN parameter [...] is included, then the size measurement of the BH shadow will [...] lead to a constraint on a linear combination of these parameters.” However, the combination in question is nothing but b_{ph} itself (as shown by the solid and dashed lines in Fig. 2), and becomes linear only if deviations of the PN coefficients from their GR values are small (which is not obvious). Under this

⁵ We assume here a 5% precision for the shadow-size measurement, which may be achievable with next-generation EHT-like experiments [66], to show that these conclusions will not change with better future data.

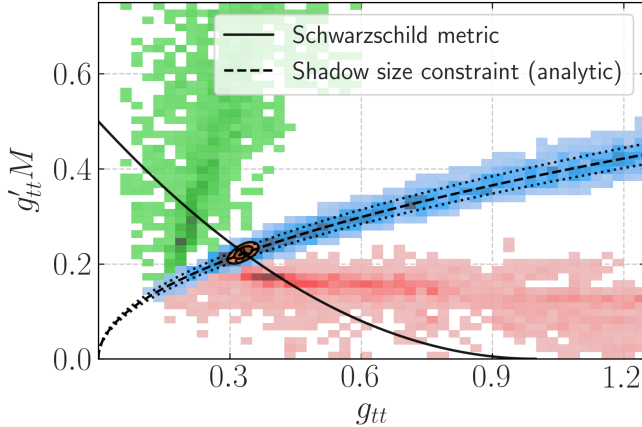


FIG. 2. Posteriors for g_{tt} and g'_{tt} , produced by our MCMC sampler in the case of shadow-size measurement with 5% error, and five free parameters $\epsilon, a_0, a_1, a_2, a_3$. The posteriors are evaluated at $r = r_{\text{ph}}$ (blue), $r = 0.85 r_{\text{ph}}$ (green) and $r = 1.15 r_{\text{ph}}$ (red). Analytic predictions for g_{tt} and g'_{tt} at r_{ph} [from Eqs. (6) and (7)] are provided by the black dashed line and by the black dotted ones (1 σ error bars). For comparison, the Schwarzschild metric is shown for $r \in [2M, \infty]$ (black solid). To demonstrate the close relation between QNM and shadow-size measurements, we also show the MCMC results assuming a $l = 2, n = 0$ QNM measured with 5% accuracy (orange), using the code of Ref. [67].

assumption, however, one can solve Eqs. (6)–(7) by inserting the PN metric (3) and linearizing in the P_i . One then obtains that the EHT bound is approximately (at 68% confidence and assuming vanishing BH spin)

$$\frac{1}{2} \left| \sum_{i=1}^{\infty} \frac{P_i}{3^i} \right| \lesssim 0.17. \quad (11)$$

We stress that the coefficients of this combination will be different for non-vanishing spin. In fact, since for high spins the circular photon orbit approaches (in Boyer-Lindquist coordinates) the horizon [53], we expect those coefficients to all be comparable.

This approximate constraint explains the growing width of the “optimistic” bounds of Fig. 1 as the PN order increases. It also suggests that bounds on the lowest-order PN parameters (0PN [13] and -1PN [14, 59]) from GW observations of the early inspiral of BH binaries are potentially stronger than those from shadow-size measurements, even though posterior correlations may still appear at higher-PN orders, when several parameters are varied at the same time [13, 68]. In more detail, GW detectors are sensitive to a whole time (or frequency) series, unlike the EHT shadow-size observation (which amounts to a single data point). They measure, in particular, the GW phase $\Phi(f) = \Phi_{\text{GR}}(f)[\sum_{i=-1}^{\infty} \delta_i(Mf)^{2i/3}]$, where $\Phi_{\text{GR}}(f)$ is the GR-predicted phase, f the GW frequency, M the binary total mass, and the δ_i are parameters accounting for deviations from GR at (integer) PN

orders [13, 14, 55, 57, 69–71] (in the GR limit, $\delta_0 = 1$ and $\delta_i = 0$ for $i > 0$). Since $(Mf)^{2/3} \propto M/r$ (with r the orbital separation), the phase is a series in M/r , just like Eq. (11). The difference with Eq. (11) is that BH-binary inspiral observations are sensitive to separations from tens of M down to $\sim 6M$, which accelerates convergence. Similarly, X-ray observations of accretion disks around BHs [55, 72–75] are sensitive to radii larger than the innermost stable circular orbit, thus being in a regime where the PN expansion is applicable (although bounds derived from these observations may depend on the accretion-disk model [32, 76, 77]).

An alternative way to exploit EHT observations is to consider BH solutions in gravitational theories different from GR, which are often known exactly and/or numerically and which will in general show deviations from the Schwarzschild/Kerr metric at all PN orders. To show this explicitly, we will present a few examples, making (like above) the simplifying assumption of spherical symmetry.⁶ Consider first the Reissner-Nordström-like BH of Eq. (10). If $\alpha_1 = 0$, that reduces exactly to the Reissner-Nordström spacetime, which features $P_i = 0$ for $i \geq 2$. The EHT shadow-size measurement then bounds $P_1 \propto Q^2$ in the 68% confidence interval $[0, 0.81]$. In the general case, the solution is governed by two independent parameters: the coupling α_1 and the BH charge Q . The fractional difference between b_{ph} and the Schwarzschild value is shown in Fig. 3, with the region within the 17% contour being in agreement with the EHT shadow-size measurement. From these bounds, one may then obtain posteriors for the PN coefficients, whose 68% confidence intervals are $P_1 \in [-1.04, 0.81]$, $P_2 \in [-0.90, 0.12]$, $P_3 \in [-1.40, 0.053]$, $P_4 \in [-2.48, 0.031]$.

Hairy BHs differing from the Schwarzschild one can also be obtained in scalar-tensor theories, provided that a coupling between the scalar ϕ and the Gauss-Bonnet invariant $\mathcal{G} = R^{abcd}R_{abcd} - 4R^{ab}R_{ab} + R^2$ is introduced, giving rise to theories known as Einstein-scalar-Gauss-Bonnet gravity. Their action is [78]

$$S = \int \frac{d^4x \sqrt{-g}}{16\pi} \left[R - \frac{1}{2} \nabla_a \phi \nabla^a \phi + \lambda^2 f(\phi) \mathcal{G} \right], \quad (12)$$

with λ a coupling constant (with dimensions of a length) and $f(\phi)$ a dimensionless coupling function. Provided that $f(\phi)$ is monotonic, one can find BH solutions characterized by a dimensionless scalar charge, defined from the decay $\phi \simeq \phi_\infty + qM/r$ of the scalar near spatial infinity, being M the BH mass and ϕ_∞ the asymptotic value of

⁶ Such a theory-by-theory approach is not needed in situations where the PN expansion is well suited for the system at hand and yields robust bounds. This is the case e.g. for solar-system tests, for which parametric bounds on the 1PN coefficients are robust and can be readily converted into constraints on specific theories.

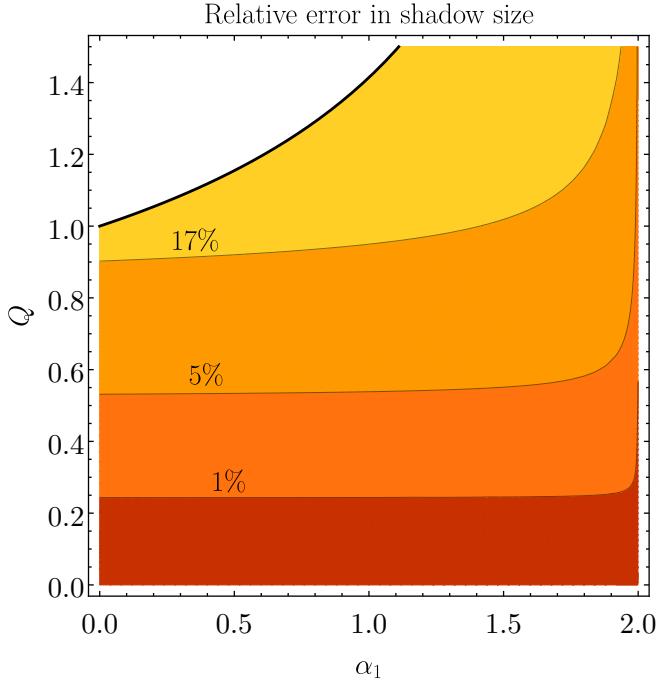


FIG. 3. Relative difference between the shadow size of a BH in Einstein-Maxwell-dilaton gravity and a Schwarzschild BH with the same mass. Contours correspond to differences of 1%, 5% and 17% (from darker to lighter regions). The solid black line represents extremal solutions. Reissner-Nordström solutions lie on the line $\alpha_1 = 0$.

the scalar field. For these theories $q = \lambda^2 f'(\phi_\infty)/(2M^2)$, where a prime denotes the derivative with respect to ϕ . Numerical solutions can be found for specific coupling functions, e.g. $f(\phi) = \exp(\phi)$ [79, 80], or $f(\phi) \propto \phi$ [81, 82]. Alternatively, one can find solutions perturbatively in the charge q for various monotonic coupling functions [78, 83–85]. Using the fits of [86] to the numerical solutions of [79] [for $f(\phi) = \exp(\phi)$], we find that these BHs always agree with the EHT shadow-size measurement if the precision of the measurement is worse than $\sim 1\%$. This confirms the findings of [42].

Interesting solutions can also be found for non-monotonic coupling functions. If $f(\phi)$ has a minimum, BHs can scalarize spontaneously in Einstein-scalar-Gauss-Bonnet gravity [44, 87–92]. These scalarized BHs form because the Schwarzschild and/or Kerr solutions of GR become tachyonically unstable in these theories [87, 88, 93–97].

Consider the case $f(\phi) = [1 - \exp(-6\phi^2)]/12$, studied in [44, 88]. This theory provides a continuum set of scalarized BHs with mass $M \in [0, 0.587\lambda]$. The EHT shadow-size measurement then constrains $\lambda < 3.27M$ (see also [44])⁷. While this bound is not new (having

been derived in [44], cf. their Fig. 5), one can compare it with the results of our Fig. 1 for the RZ parametrized metric. The PN expansion of scalarized BHs (obtained by solving the field equations perturbatively near spatial infinity) yields PN parameters $P_1 = 0$, $P_2 = q^2/3$, $P_3 = 2q^2/3$, $P_4 = 6q^2/5 - 3q^4/20 + 16q^2\lambda^2/5M^2$. Moreover, an additional coupling of the scalar to the Ricci curvature can even give rise to $P_1 \neq 0$ [98]. The charge q is a function of λ , and can be extracted from the numerical solutions to the full field equations. The EHT bound $\lambda/M < 3.27$ then translates into the constraint $q < 0.195$ and thus $|P_2| < 0.136$, $|P_3| < 0.272$, $|P_4| < 14.46$. As can be seen, in this specific case the bounds on the PN parameters are comparable to (or even better than) the “optimistic” bounds of Fig. 1.

Discussion: We stress that the dependence of the shadow-size bounds on the PN coefficients on how many of them are allowed to vary, as well as the robustness of the constraints on the geometry near the circular photon orbit are reminiscent of what happens with GW observations of QNMs in the ringdown phase of binary BHs. Indeed, shadow-size measurements are to the EHT what QNMs are to GW detectors. Both shadows and QNMs are sensitive to the BH geometry near the circular photon orbit, and their physics cannot be described within the PN approximation. Note that [67] attempted to constrain parametrized metrics (e.g. the RZ metric) with QNM observations. In agreement with this letter, [67] found that constraints on the reconstructed geometry are robust near the peak of the effective potential. We show this explicitly in Fig. 2, where we present projected QNM constraints on g_{tt} and dg_{tt}/dr , alongside those from the shadow size mentioned earlier, in the “pessimistic” case where the four non-zero parameters ϵ , a_1 , a_2 and a_3 are allowed to vary simultaneously.

In more detail, the geometric-optics limit of the GW propagation equation reduces, in GR, to the null-geodesics one (see e.g., [67]), i.e., high-frequency gravitational wavefronts follow null geodesics. Therefore, the effective potential for QNMs in the geometric-optics limit (i.e., the limit of large angular eigen-numbers ℓ, m) coincides with that of null geodesics [Eq. (4)]. Since QNMs are generated at the peak of the effective potential, which is close to the circular photon orbit (and coincides with it for $\ell \gtrsim m \gg 1$), it is not surprising that the QNM frequencies of the Kerr spacetime are given (in the geometric-optics limit) by linear combinations of the orbital and frame-dragging precession frequencies of the circular null orbit (or simply by multiples of the orbital frequency in Schwarzschild, where the two frequencies coincide) [99–102]. Similarly, one can relate QNM decay times to the Lyapunov exponents of null geodesics near

⁷ We expect $\lambda \gg 100M_\odot$ to agree with early-inspiral GW obser-

vations (because $q \rightarrow 0$ as $M/\lambda \sim 0$: cf. [88], Fig. 4), although merger/ringdown bounds have not been derived yet.

the circular photon orbit [100–103]. These exponents depend in turn on the curvature of the effective potential for photon orbits near its peak.

This null geodesics/QNMs correspondence can be generalized to BH spacetimes different from Kerr/Schwarzschild, at least in a wide class of gravitational theories [67, 104–106]. This correspondence motivates combining EHT shadow-size tests of the no-hair theorem with the QNM null tests of the same theorem that will become possible with third-generation GW interferometers or spaced-based detectors such as e.g., LISA [24] or TianQin [107].

Acknowledgments: S.V., E.B. and N.F. acknowledge financial support provided under the European Union’s H2020 ERC Consolidator Grant “GRavity from Astrophysical to Microscopic Scales” grant agreement no. GRAMS-815673. This work was supported in part by Perimeter Institute for Theoretical Physics. Research at Perimeter Institute is supported by the Government of Canada through the Department of Innovation, Science and Economic Development Canada and by the Province of Ontario through the Ministry of Economic Development, Job Creation and Trade. A.E.B. thanks the Delaney Family for their generous financial support via the Delaney Family John A. Wheeler Chair at Perimeter Institute. A.E.B. and receives additional financial support from the Natural Sciences and Engineering Research Council of Canada through a Discovery Grant. We thank A. Cardenas Avendano, E. Berti, K. Glampedakis, R. Gold, P. Kocherlakota, K. D. Kokkotas, L. Rezzolla, N. Wex and N. Yunes for insightful conversations and for reviewing a draft of this manuscript. During the completion of this work we have become aware of a related work by P. Kocherlakota, L. Rezzolla, *et al.*, which deals with topics that partly overlap with those of this manuscript (i.e. EHT bounds on exact non-GR BH solutions).

L3 (2020).

- [7] R. Abbott *et al.* (LIGO Scientific, Virgo), (2020), arXiv:2004.08342 [astro-ph.HE].
- [8] R. Abbott *et al.* (LIGO Scientific, Virgo), *Astrophys. J. Lett.* **896**, L44 (2020), arXiv:2006.12611 [astro-ph.HE].
- [9] R. Abbott *et al.* (LIGO Scientific, Virgo), *Phys. Rev. Lett.* **125**, 101102 (2020), arXiv:2009.01075 [gr-qc].
- [10] C. M. Will, *Theory and Experiment in Gravitational Physics* (Cambridge University Press, 2018).
- [11] T. Damour and J. H. Taylor, *Phys. Rev. D* **45**, 1840 (1992).
- [12] L. Blanchet, *Living Rev. Rel.* **17**, 2 (2014), arXiv:1310.1528 [gr-qc].
- [13] B. P. Abbott and et al. (LIGO Scientific and Virgo Collaborations), *Phys. Rev. Lett.* **116**, 221101 (2016).
- [14] B. Abbott *et al.* (LIGO Scientific, Virgo), *Phys. Rev. D* **100**, 104036 (2019), arXiv:1903.04467 [gr-qc].
- [15] R. Abbott *et al.* (LIGO Scientific, Virgo), (2020), arXiv:2010.14529 [gr-qc].
- [16] K. D. Kokkotas and B. G. Schmidt, *Living Rev. Rel.* **2**, 2 (1999), arXiv:gr-qc/9909058.
- [17] H.-P. Nollert, *Classical and Quantum Gravity* **16**, R159 (1999).
- [18] E. Berti, V. Cardoso, and A. O. Starinets, *Classical and Quantum Gravity* **26**, 163001 (2009).
- [19] W. Israel, *Phys. Rev.* **164**, 1776 (1967).
- [20] S. Hawking, *Commun. Math. Phys.* **25**, 152 (1972).
- [21] B. Carter, *Phys. Rev. Lett.* **26**, 331 (1971).
- [22] D. Robinson, *Phys. Rev. Lett.* **34**, 905 (1975).
- [23] O. Dreyer, B. J. Kelly, B. Krishnan, L. S. Finn, D. Garrison, and R. Lopez-Aleman, *Class. Quant. Grav.* **21**, 787 (2004), arXiv:gr-qc/0309007.
- [24] E. Berti, A. Sesana, E. Barausse, V. Cardoso, and K. Belczynski, *Phys. Rev. Lett.* **117**, 101102 (2016), arXiv:1605.09286 [gr-qc].
- [25] M. Giesler, M. Isi, M. A. Scheel, and S. Teukolsky, *Phys. Rev. X* **9**, 041060 (2019), arXiv:1903.08284 [gr-qc].
- [26] D. Psaltis *et al.* (EHT Collaboration), *Phys. Rev. Lett.* **125**, 141104 (2020).
- [27] K. Akiyama *et al.* (Event Horizon Telescope), *Astrophys. J. Lett.* **875**, L5 (2019), arXiv:1906.11242 [astro-ph.GA].
- [28] S. E. Gralla, D. E. Holz, and R. M. Wald, *Phys. Rev. D* **100**, 024018 (2019), arXiv:1906.00873 [astro-ph.HE].
- [29] S. E. Gralla, (2020), arXiv:2010.08557 [astro-ph.HE].
- [30] K. Akiyama *et al.* (Event Horizon Telescope), *Astrophys. J.* **875**, L1 (2019), arXiv:1906.11238 [astro-ph.GA].
- [31] K. Akiyama *et al.* (Event Horizon Telescope), *Astrophys. J. Lett.* **875**, L6 (2019), arXiv:1906.11243 [astro-ph.GA].
- [32] A. Cardenas-Avendano, J. Godfrey, N. Yunes, and A. Lohfink, *Phys. Rev. D* **100**, 024039 (2019), arXiv:1903.04356 [gr-qc].
- [33] R. Takahashi, *Publ. Astron. Soc. Jap.* **57**, 273 (2005), arXiv:astro-ph/0505316.
- [34] T. Johannsen and D. Psaltis, *Astrophys. J.* **718**, 446 (2010), arXiv:1005.1931 [astro-ph.HE].
- [35] D. Psaltis and T. Johannsen, *J. Phys. Conf. Ser.* **283**, 012030 (2011), arXiv:1012.1602 [astro-ph.HE].
- [36] L. Amarilla and E. F. Eiroa, *Phys. Rev. D* **85**, 064019 (2012), arXiv:1112.6349 [gr-qc].
- [37] A. E. Broderick, T. Johannsen, A. Loeb, and D. Psaltis,

* svoelkel@sissa.it

† barausse@sissa.it

‡ nfranchi@sissa.it

§ abroderick@perimeterinstitute.ca

- [1] B. P. Abbott and et al. (LIGO Scientific Collaboration and Virgo Collaboration), *Phys. Rev. Lett.* **116**, 061102 (2016).
- [2] B. P. Abbott and et al. (LIGO Scientific Collaboration and Virgo Collaboration), *Phys. Rev. Lett.* **116**, 241103 (2016).
- [3] B. P. Abbott and et al. (LIGO Scientific and Virgo Collaboration), *Phys. Rev. Lett.* **118**, 221101 (2017).
- [4] B. P. Abbott and et al., *The Astrophysical Journal* **851**, L35 (2017).
- [5] B. P. Abbott and et al. (LIGO Scientific Collaboration and Virgo Collaboration), *Phys. Rev. Lett.* **119**, 141101 (2017).
- [6] B. P. Abbott and et al., *The Astrophysical Journal* **892**,

- Astrophys. J.* **784**, 7 (2014), arXiv:1311.5564 [astro-ph.HE].
- [38] D. Psaltis, F. Ozel, C.-K. Chan, and D. P. Marrone, *Astrophys. J.* **814**, 115 (2015), arXiv:1411.1454 [astro-ph.HE].
- [39] T. Johannsen, A. E. Broderick, P. M. Plewa, S. Chatzopoulos, S. S. Doeleman, F. Eisenhauer, V. L. Fish, R. Genzel, O. Gerhard, and M. D. Johnson, *Phys. Rev. Lett.* **116**, 031101 (2016), arXiv:1512.02640 [astro-ph.GA].
- [40] D. Psaltis, N. Wex, and M. Kramer, *Astrophys. J.* **818**, 121 (2016), arXiv:1510.00394 [astro-ph.HE].
- [41] P. V. P. Cunha, C. A. R. Herdeiro, E. Radu, and H. F. Runarsson, *Phys. Rev. Lett.* **115**, 211102 (2015), arXiv:1509.00021 [gr-qc].
- [42] P. V. Cunha, C. A. R. Herdeiro, B. Kleihaus, J. Kunz, and E. Radu, *Phys. Lett. B* **768**, 373 (2017), arXiv:1701.00079 [gr-qc].
- [43] D. Psaltis, *Gen. Rel. Grav.* **51**, 137 (2019), arXiv:1806.09740 [astro-ph.HE].
- [44] P. V. Cunha, C. A. R. Herdeiro, and E. Radu, *Phys. Rev. Lett.* **123**, 011101 (2019), arXiv:1904.09997 [gr-qc].
- [45] L. Medeiros, D. Psaltis, and F. Özel, *Astrophys. J.* **896**, 7 (2020), arXiv:1907.12575 [astro-ph.HE].
- [46] T. Johannsen and D. Psaltis, *Phys. Rev. D* **83**, 124015 (2011), arXiv:1105.3191 [gr-qc].
- [47] T. Johannsen, *Phys. Rev. D* **87**, 124017 (2013).
- [48] S. Vigeland, N. Yunes, and L. C. Stein, *Phys. Rev. D* **83**, 104027 (2011).
- [49] T. Johannsen, *Phys. Rev. D* **88**, 044002 (2013).
- [50] L. Rezzolla and A. Zhidenko, *Phys. Rev. D* **90**, 084009 (2014).
- [51] R. Konoplya, L. Rezzolla, and A. Zhidenko, *Phys. Rev. D* **93**, 064015 (2016), arXiv:1602.02378 [gr-qc].
- [52] Z. Younsi, A. Zhidenko, L. Rezzolla, R. Konoplya, and Y. Mizuno, *Phys. Rev. D* **94**, 084025 (2016), arXiv:1607.05767 [gr-qc].
- [53] J. Bardeen, in *Les Houches Summer School of Theoretical Physics: Black Holes* (1973) pp. 215–240.
- [54] J. Salvatier, T. V. Wiecki, and C. Fonnesbeck, *PeerJ Computer Science* **2**, e55 (2016).
- [55] A. Cardenas-Avendano, S. Nampalliwar, and N. Yunes, *Class. Quant. Grav.* **37**, 135008 (2020), arXiv:1912.08062 [gr-qc].
- [56] L. Sampson, N. Cornish, and N. Yunes, *Phys. Rev. D* **87**, 102001 (2013), arXiv:1303.1185 [gr-qc].
- [57] N. Yunes, K. Yagi, and F. Pretorius, *Phys. Rev. D* **94**, 084002 (2016), arXiv:1603.08955 [gr-qc].
- [58] D. Psaltis, C. Talbot, E. Payne, and I. Mandel, *Phys. Rev. D* **103**, 104036 (2021), arXiv:2012.02117 [gr-qc].
- [59] E. Barausse, N. Yunes, and K. Chamberlain, *Phys. Rev. Lett.* **116**, 241104 (2016), arXiv:1603.04075 [gr-qc].
- [60] E. Berti *et al.*, *Class. Quant. Grav.* **32**, 243001 (2015), arXiv:1501.07274 [gr-qc].
- [61] D. Garfinkle, G. T. Horowitz, and A. Strominger, *Phys. Rev. D* **43**, 3140 (1991), [Erratum: Phys.Rev.D 45, 3888 (1992)].
- [62] E. W. Hirschmann, L. Lehner, S. L. Liebling, and C. Palenzuela, *Phys. Rev. D* **97**, 064032 (2018), arXiv:1706.09875 [gr-qc].
- [63] S. D. McDermott and S. J. Witte, *Phys. Rev. D* **101**, 063030 (2020), arXiv:1911.05086 [hep-ph].
- [64] G. Gibbons and K.-i. Maeda, *Nucl. Phys. B* **298**, 741 (1988).
- [65] E. Barausse, V. Cardoso, and P. Pani, *Phys. Rev. D* **89**, 104059 (2014), arXiv:1404.7149 [gr-qc].
- [66] A. W. Raymond, D. Palumbo, S. N. Paine, L. Blackburn, R. Córdova Rosado, S. S. Doeleman, J. R. Farah, M. D. Johnson, F. Roelofs, R. P. J. Tilanus, and J. Weintraub, *Astrophys. J. Suppl.* **253**, 5 (2021), arXiv:2102.05482 [astro-ph.IM].
- [67] S. H. Völkel and E. Barausse, *Phys. Rev. D* **102**, 084025 (2020), arXiv:2007.02986 [gr-qc].
- [68] A. A. Shoom, P. K. Gupta, B. Krishnan, A. B. Nielsen, and C. D. Capano, (2021), arXiv:2105.02191 [gr-qc].
- [69] N. Yunes and F. Pretorius, *Phys. Rev. D* **80**, 122003 (2009), arXiv:0909.3328 [gr-qc].
- [70] N. Cornish, L. Sampson, N. Yunes, and F. Pretorius, *Phys. Rev. D* **84**, 062003 (2011), arXiv:1105.2088 [gr-qc].
- [71] K. Chatzioannou, N. Yunes, and N. Cornish, *Phys. Rev. D* **86**, 022004 (2012), [Erratum: Phys.Rev.D 95, 129901 (2017)], arXiv:1204.2585 [gr-qc].
- [72] C. Bambi and E. Barausse, *Astrophys. J.* **731**, 121 (2011), arXiv:1012.2007 [gr-qc].
- [73] C. Bambi, *Rev. Mod. Phys.* **89**, 025001 (2017), arXiv:1509.03884 [gr-qc].
- [74] A. Tripathi, A. B. Abdikamalov, D. Ayzenberg, C. Bambi, and S. Nampalliwar, *Phys. Rev. D* **99**, 083001 (2019), arXiv:1903.04071 [gr-qc].
- [75] S. Nampalliwar, S. Xin, S. Srivastava, A. B. Abdikamalov, D. Ayzenberg, C. Bambi, T. Dauser, J. A. Garcia, and A. Tripathi, (2019), arXiv:1903.12119 [gr-qc].
- [76] S. Riaz, D. Ayzenberg, C. Bambi, and S. Nampalliwar, *Mon. Not. Roy. Astron. Soc.* **491**, 417 (2020), arXiv:1908.04969 [astro-ph.HE].
- [77] A. B. Abdikamalov, D. Ayzenberg, C. Bambi, T. Dauser, J. A. Garcia, S. Nampalliwar, A. Tripathi, and M. Zhou, *Astrophys. J.* **899**, 80 (2020), arXiv:2003.09663 [astro-ph.HE].
- [78] F.-L. Julié and E. Berti, *Phys. Rev. D* **100**, 104061 (2019), arXiv:1909.05258 [gr-qc].
- [79] P. Kanti, N. Mavromatos, J. Rizos, K. Tamvakis, and E. Winstanley, *Phys. Rev. D* **54**, 5049 (1996), arXiv:hep-th/9511071.
- [80] P. Pani and V. Cardoso, *Phys. Rev. D* **79**, 084031 (2009), arXiv:0902.1569 [gr-qc].
- [81] T. P. Sotiriou and S.-Y. Zhou, *Phys. Rev. Lett.* **112**, 251102 (2014), arXiv:1312.3622 [gr-qc].
- [82] T. P. Sotiriou and S.-Y. Zhou, *Phys. Rev. D* **90**, 124063 (2014), arXiv:1408.1698 [gr-qc].
- [83] S. Mignemi and N. Stewart, *Phys. Rev. D* **47**, 5259 (1993), arXiv:hep-th/9212146.
- [84] N. Yunes and L. C. Stein, *Phys. Rev. D* **83**, 104002 (2011), arXiv:1101.2921 [gr-qc].
- [85] A. Maselli, P. Pani, L. Gualtieri, and V. Ferrari, *Phys. Rev. D* **92**, 083014 (2015), arXiv:1507.00680 [gr-qc].
- [86] K. Kokkotas, R. Konoplya, and A. Zhidenko, *Phys. Rev. D* **96**, 064004 (2017), arXiv:1706.07460 [gr-qc].
- [87] H. O. Silva, J. Sakstein, L. Gualtieri, T. P. Sotiriou, and E. Berti, *Phys. Rev. Lett.* **120**, 131104 (2018), arXiv:1711.02080 [gr-qc].
- [88] D. Doneva and S. S. Yazadjiev, *Phys. Rev. Lett.* **120**, 131103 (2018), arXiv:1711.01187 [gr-qc].
- [89] G. Antoniou, A. Bakopoulos, and P. Kanti, *Phys. Rev. Lett.* **120**, 131102 (2018), arXiv:1711.03390 [hep-th].
- [90] L. G. Collodel, B. Kleihaus, J. Kunz, and

- E. Berti, *Class. Quant. Grav.* **37**, 075018 (2020), [arXiv:1912.05382 \[gr-qc\]](#).
- [91] C. A. Herdeiro, E. Radu, H. O. Silva, T. P. Sotiriou, and N. Yunes, (2020), [arXiv:2009.03904 \[gr-qc\]](#).
- [92] E. Berti, L. G. Collodel, B. Kleihaus, and J. Kunz, (2020), [arXiv:2009.03905 \[gr-qc\]](#).
- [93] N. Andreou, N. Franchini, G. Ventagli, and T. P. Sotiriou, *Phys. Rev. D* **99**, 124022 (2019), [Erratum: Phys.Rev.D 101, 109903 (2020)], [arXiv:1904.06365 \[gr-qc\]](#).
- [94] M. Minamitsuji and T. Ikeda, *Phys. Rev. D* **99**, 104069 (2019), [arXiv:1904.06572 \[gr-qc\]](#).
- [95] A. Dima, E. Barausse, N. Franchini, and T. P. Sotiriou, (2020), [arXiv:2006.03095 \[gr-qc\]](#).
- [96] D. D. Doneva, L. G. Collodel, C. J. Krüger, and S. S. Yazadjiev, (2020), [arXiv:2008.07391 \[gr-qc\]](#).
- [97] D. D. Doneva, L. G. Collodel, C. J. Krüger, and S. S. Yazadjiev, (2020), [arXiv:2009.03774 \[gr-qc\]](#).
- [98] G. Antoniou, A. Lehébel, G. Ventagli, and T. P. Sotiriou, (2021), [arXiv:2105.04479 \[gr-qc\]](#).
- [99] C. J. Goebel, *Astrophys. J. Lett.* **172**, L95 (1972).
- [100] V. Ferrari and B. Mashhoon, *Phys. Rev. D* **30**, 295 (1984).
- [101] B. F. Schutz and C. M. Will, *Astrophys. J. Lett.* **291**, L33 (1985).
- [102] H. Yang, D. A. Nichols, F. Zhang, A. Zimmerman, Z. Zhang, and Y. Chen, *Physical Review D* **86** (2012), 10.1103/physrevd.86.104006.
- [103] V. Cardoso, A. S. Miranda, E. Berti, H. Witek, and V. T. Zanchin, *Phys. Rev. D* **79**, 064016 (2009), [arXiv:0812.1806 \[hep-th\]](#).
- [104] K. Glampedakis, G. Pappas, H. O. Silva, and E. Berti, *Physical Review D* **96** (2017), 10.1103/physrevd.96.064054.
- [105] K. Glampedakis and H. O. Silva, *Phys. Rev. D* **100**, 044040 (2019), [arXiv:1906.05455 \[gr-qc\]](#).
- [106] H. O. Silva and K. Glampedakis, *Phys. Rev. D* **101**, 044051 (2020), [arXiv:1912.09286 \[gr-qc\]](#).
- [107] C. Shi, J. Bao, H. Wang, J.-d. Zhang, Y. Hu, A. Sesana, E. Barausse, J. Mei, and J. Luo, *Phys. Rev. D* **100**, 044036 (2019), [arXiv:1902.08922 \[gr-qc\]](#).